Experimental intercomparison of the absorption cross-sections of nitrous acid (HONO) in the ultraviolet and mid-infrared spectral regions

ARTICLE *in* JOURNAL OF QUANTITATIVE SPECTROSCOPY AND RADIATIVE TRANSFER · MARCH 2009

Impact Factor: 2.65 · DOI: 10.1016/j.jqsrt.2008.11.003

Journal of Quantitative Spectroscopy & Radiative Transfer ▮ (▮▮▮▮) ▮▮▮–▮▮▮

Contents lists available at ScienceDirect

Journal of Quantitative Spectroscopy & Radiative Transfer

journal homepage: www.elsevier.com/locate/jqsrt

Experimental intercomparison of the absorption cross-sections of nitrous acid (HONO) in the ultraviolet and mid-infrared spectral regions

A. Gratien *, M. Lefort, B. Picquet-Varrault, J. Orphal, J.-F. Doussin, J.-M. Flaud

Laboratoire Interuniversitaire des Systèmes Atmosphériques (LISA), UMR CNRS 7583, Universities Paris 12 (Paris-Est) and Paris 7, 61 Avenue du Général de Gaulle, 94010 Créteil, France

ARTICLE INFO

Article history:
Received 4 August 2008
Received in revised form
2 November 2008
Accepted 4 November 2008

Keywords:
Absorption cross-sections
Infrared
Ultraviolet
Nitrous acid
HONO

ABSTRACT

Nitrous acid, HONO, is an important trace gas in tropospheric photochemistry, because it is a source of OH radicals. In order to obtain HONO concentrations from spectroscopic measurements, the knowledge of accurate absorption cross-sections is essential. Furthermore, the ultraviolet absorption cross-sections of HONO determine its atmospheric photolysis rates, which are still being debated. In particular, in a recent field study focusing on the photolysis frequency of HONO, the absolute values of the ultraviolet absorption cross-sections have been proposed as a potential source for systematic errors. For these reasons, we have compared the absorption cross-sections for HONO in the infrared (IR) and ultraviolet (UV) by performing simultaneous measurements in both spectral regions. Assuming that the IR cross-sections (that show good agreement between different studies) are correct, our study shows a good agreement between the consistent infrared studies and some selected accurate UV spectra published previously (about 6%) while a rather large disagreement (about 22%) is observed when using other UV data sets.

1. Introduction

Nitrous acid, HONO, is an important trace gas in tropospheric photochemistry. HONO has been observed to accumulate through the night, with concentrations occasionally as high as 15 ppb, and its photolysis (Eq. (1)) enhances photo-oxidation processes in the morning due to the production of OH radicals, at a time of the day when other sources of OH (e.g., photolysis of O_3 and HCHO) are still small [1–3]:

$$\mathrm{HONO} + h\nu \rightarrow \mathrm{NO} + \mathrm{OH} \quad (300\,\mathrm{nm} < \lambda < 405\,\mathrm{nm}) \tag{1}$$

Recently, field studies have demonstrated the important role of HONO as OH radical source in the morning, when photolysis starts, but also throughout the entire day indicating the existence of a strong daytime source [4,5].

Rural concentrations of HONO are on average around 0.6 ppb, but with daily maxima in winter up to 8 ppb [6]. The highest HONO concentrations are generally observed in polluted areas due to high concentrations of the precursor species NO_2. For example, HONO concentrations of up to 10 ppb have been observed in Milan, Italy [7], and in the Los Angeles area [8]. Inside vehicles, HONO concentrations can even attain values as high as 40 ppb [9].

* Corresponding author. Tel.: +33 01 45 17 15 88; fax: +33 01 45 17 15 64.
E-mail address: aline.gratien@lisa.univ-paris12.fr (A. Gratien).

0022-4073/$ - see front matter © 2008 Elsevier Ltd. All rights reserved.
doi:10.1016/j.jqsrt.2008.11.003

Despite the importance of HONO in atmospheric chemistry, the sources of tropospheric HONO and the detailed chemical mechanisms for its production are still not well understood [9–11]. In particular, modelled HONO concentrations taking into account only the gas-phase chemistry do not reproduce the observed values [12]. Thus, HONO is suggested to be formed by both homogeneous [13,14] and heterogeneous processes [9,15–18]. For example, heterogeneous reactions on soot [19,20], on secondary organic aerosol [21] have been studied. In these studies, HONO formation on organic aerosols [21] and on soot [20] was also excluded. In addition, the photo-sensitized formation of HONO on humic acid aerosol [22,23] and the photochemical formation by the nitrate photolysis [24] has been proposed. The heterogeneous formation between NO_2 and the aromatics has been also investigated to explain the source of HONO during the day [25,26]. Very recently, the gas-phase reaction of electronically excited NO_2 with H_2O was proposed as significant gas-phase source of HONO during the day [27,28].

In this context, accurate measurements of tropospheric HONO concentrations are particularly important. Atmospheric HONO concentrations have been measured with various spectroscopic and chemical techniques. HONO was observed for the first time in the atmosphere in the late 1970s using differential optical absorption spectroscopy (DOAS) [8,29,30]. Note that atmospheric HONO concentrations can also be measured with other spectroscopic techniques, including cavity ring down spectroscopy (CRDS) and cavity-enhanced absorption spectroscopy (CEAS) [31,32], Fourier transform spectroscopy (FTS) [33,34], tuneable diode laser spectroscopy (TDLS) [35] and photo-fragmentation followed by laser-induced fluorescence (PF/LIF) detection [36]. Among the spectroscopic techniques, DOAS is the most usually employed [8,17,29,30,37]. On the other hand, nitrous acid has also been measured by chemistry techniques: denuder methods [7,9,38–42], diffusion scrubber [1,43–46]. More recently, a new sensitive measurement technique (long-path absorption photometer), "LOPAP" [47,48], has been developed that uses wet chemical sampling and photometric detection. While chemical instruments can be affected quite significantly by interferences and sampling artefacts, spectroscopic techniques are generally free of sampling artefacts and of chemical interferences, but often less sensitive than the chemical instruments, and have to deal with overlapping spectra of interfering species.

To validate atmospheric HONO measurements, several intercomparisons of different *in-situ* techniques have been performed in field campaigns, in particular between the two most commonly used methods, i.e., the DOAS and the chemical denuder techniques [7,42,49]. Moreover, the LOPAP technique was validated against the DOAS technique [47,48]. The results show good agreement [48] or significant differences [47] which are, however, explained by an NO_2 artefact of the DOAS instrument [44].

Since DOAS is the technique most usually employed to measure atmospheric HONO using its electronic bands (300–400 nm), accurate knowledge of its UV absorption cross-sections is of the utmost importance. The UV absorption cross-sections of HONO have been measured by different authors; however, systematic differences of up to 26% are observed between different recent studies [50–53].

On the other hand, the first IR/UV intercomparison of Barney et al. [54,55] has shown a good agreement between (i) the different published IR absorption cross-sections [56–58] except for the study of Chan et al. [14] (cf. Table 1) and (ii) these IR cross-sections and the UV data of Bongartz et al. [51].

In addition to their importance for atmospheric measurements of HONO, the UV absorption cross-sections also determine the production of OH from HONO photolysis. The HONO photolysis frequency is indeed defined by

$$J_{\mathrm{HONO}} = \int \sigma_{\mathrm{HONO}}(\lambda)\phi_{\mathrm{HONO}}(\lambda)\psi(\lambda)\,\mathrm{d}\lambda \tag{2}$$

where $\psi(\lambda)$ is the spectral actinic flux, $\sigma(\lambda)$ and $\phi(\lambda)$ are, respectively, the UV absorption cross-sections and the photo-dissociation quantum yields of nitrous acid.

As a consequence a recent field study on the HONO photolysis frequencies [59] points out that the absolute values of the UV absorption cross-sections are to be considered as a potential source for systematic errors in the photolysis frequencies.

The objective of the present study is to assess the accuracy of the different HONO absorption cross-sections in the UV (300–400 nm) that have been published previously, using the available IR cross-sections of HONO in the 740–1300 cm^{-1} region as references and acquiring simultaneously UV and IR spectra using one single absorption cell.

Table 1
Integrated cross sections IBI and cross sections σ at 852 cm^{-1} of HONO.

Reference	$\sigma \times 10^{19}$(cm^2 $molecule^{-1}$)	IBI $\times 10^{17}$ (cm $molecule^{-1}$)		
	852 cm^{-1}	740–820 cm^{-1}	820–900 cm^{-1}	1220–1300 cm^{-1}
Chan et al. [14]	8.7 ± 0.9	–	–	–
Sakamaki et al. [58]	6.58	–	–	–
Kagann and Maki [57]	–	1.5 ± 0.2	1.30 ± 0.19	1.9 ± 0.2
Hurley [56]	–	1.48 ± 0.07[a]	1.43 ± 0.07[a]	2.08 ± 0.10[a]
Barney et al. [54, 55][b]	6.2 ± 0.7	1.6 ± 0.3	1.45 ± 0.14	1.9 ± 0.2

[a] Uncertainties of ≈5% were supposed.
[b] IR/UV intercomparaison with the UV spectrum of Bongartz et al. [51].

Please cite this article as: Gratien A, et al. Experimental intercomparison of the absorption cross-sections of nitrous acid (HONO) in the ultraviolet and mid-infrared spectral regions. JQSRT (2008), doi:10.1016/j.jqsrt.2008.11.003

2. Experimental

UV and IR absorption spectra were recorded simultaneously in the same absorption cell which is an evacuable Pyrex reactor (length: 6 m; volume: 977 l) at a temperature of 297 ± 2 K and in a pure nitrogen (N_2) atmosphere at atmospheric pressure (1013 ± 15 mbar). A detailed description of this set-up is given in Doussin et al. [60]. The reactor contains two White-type multiple reflection optical systems interfaced to a Fourier-transform infrared (FTIR) spectrometer and to a UV–visible grating spectrometer.

2.1. UV–visible measurements

The UV system consists of a light source (high-pressure xenon arc lamp Osram XBO, 450W Xe UV), a "divided-beam" system allowing correction of the intensity variations of the XBO lamp during the experiments by recording simultaneously the lamp spectrum outside of the absorption cell [61], a multi-pass White optics inside the reactor, a monochromator (HR 320, Jobin-Yvon) and a CCD array (CCD 3000, Jobin-Yvon) as detector. To reduce stray light in the spectrometer due to the very high intensity of the source in the visible region, a UG5 bandpass filter (Oriel) of 3 mm thickness is permanently placed in the light beam. Spectra were acquired between 300 and 400 nm with a spectral resolution of 0.18 nm. The wavelength scale of the UV–visible spectrometer was calibrated with reference to 30 emission lines of mercury, zinc, cesium and cadmium. For this study, the optical path length was set to 72 m (base length: 600 ± 1 cm).

2.2. Infrared measurements

The infrared spectra were recorded with a Fourier transform spectrometer (Bomem DA8-ME), equipped with a globar light source, a KBr beam splitter and a liquid nitrogen cooled MCT detector. The transfer optics between the FTS and the White cell were purged with pure nitrogen to reduce atmospheric absorption by H_2O and CO_2. Spectra were acquired between 740 and 1300 cm^{-1} with a spectral resolution of 0.08 cm^{-1}. The optical path length was set to 60 m (base length: 599.7 ± 1.0 cm) to achieve similar HONO optical depths in both the UV and IR regions.

2.3. Experimental procedure

The procedure followed in each experiment started by pumping the photoreactor to 8×10^{-3} mbar with simultaneous irradiation using UV fluorescent tubes around the cell for 1 h. After the acquisition of infrared and UV reference spectra, HONO was synthesized and directly introduced into the chamber. Then, UV and IR absorption spectra of nitrous acid were simultaneously recorded. Nitrous acid samples were prepared according to a method previously described in the literature [62]. The synthesis consists in adding 50 mL (drop by drop) of a 10% H_2SO_4 solution to 50 mL of a 0.1 M $NaNO_2$ solution. During the synthesis, the nitrous acid was flushed into the chamber using a flow of dry nitrogen. The HONO synthesis is carried out in the dark to avoid photolysis. Although this synthesis does not produce only HONO, since it also forms NO, NO_2 and H_2O by self-reactions [14], this is not a problem since the approach of the present study was to compare the UV and IR nitrous acid absorption coefficients by simultaneous measurements, which is independent of the absolute HONO concentrations.

3. Results

A total of 10 intercomparison experiments using different nitrous acid concentrations were performed by simultaneously acquiring UV and IR spectra. Figs. 1 and 2 show examples of these spectra.

In the IR spectra, residual H_2O bands interfere with the HONO absorption, particularly in the 1200–1300 cm^{-1} region. The subtraction of the H_2O absorption proved to be difficult even when using a reference spectrum of pure H_2O recorded under similar conditions with our set-up: the resulting spectrum still contains small residual water lines in the 1220–1300 cm^{-1} region, as shown in Fig. 1.

In the UV region, the main interference with the HONO absorption bands is caused by NO_2 which adsorbs in the same spectral range; the UV absorption coefficients of NO_2 are known with an accuracy of about 2% [63]. For the present study, the UV absorption coefficients of NO_2 recorded with the SCIAMACHY instrument were used as reference [64]. To solve the problem of overlapping UV absorbers, a numerical approach was employed using a script mode of the spectroscopic software DOASIS [65]. This software can separate spectra of chemical mixtures into spectral components (here NO_2 and HONO), and thus to extract from these spectra the concentrations of the two species using literature cross-sections [46–48,59,60], as shown in Fig. 2. It is important to stress the absence of any other absorber in the spectral range considered here, as shown by the residuals. For example, in the spectrum presented in Fig. 2, the observed concentration of NO_2 is $(1.6 \pm 0.1) \times 10^{14}$ molecule cm^{-3} using the reference cross-sections of Bogumil et al. [64]. It is important to mention that the NO_2 reference used here is free of HONO contaminations. Note that for HONO, the concentration

Please cite this article as: Gratien A, et al. Experimental intercomparison of the absorption cross-sections of nitrous acid (HONO) in the ultraviolet and mid-infrared spectral regions. JQSRT (2008), doi:10.1016/j.jqsrt.2008.11.003

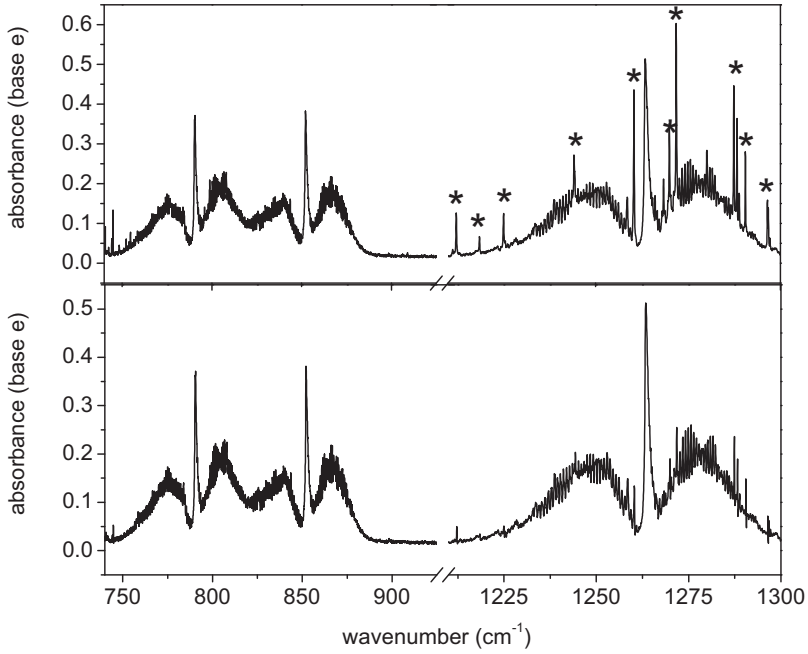

Fig. 1. Infrared spectrum of HONO (resolution: 0.08 cm^{-1}) and example of water subtraction from the spectrum. Asterisks (*) indicate position of some H_2O lines. After the subtraction, some residual water lines still remain in 1220–1300 cm^{-1} region.

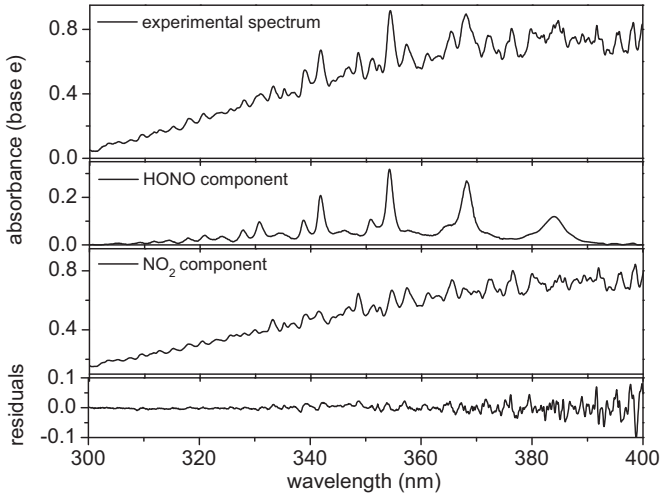

Fig. 2. Ultraviolet spectrum of a HONO/NO_2 mixture (resolution: 0.18 nm) and example of DOASIS analysis, using the NO_2 reference spectrum published by Bogumil et al. [64] and the HONO reference spectrum published by Bongartz et al. [51]. This software separates mixed spectra into components, here NO_2 and HONO, and determines from the spectra of the literature cross-sections the concentrations of these two species. In this spectrum, there are $[HONO] = (8.00 \pm 0.07) \times 10^{13}$ molecule cm^{-3} and $[NO_2] = (1.6 \pm 0.1) \times 10^{14}$ molecule cm^{-3}. Note the absence of any other absorber in this spectral range as observed in the residual.

(in the spectrum presented in Fig. 2) is

- $(8.00 \pm 0.07) \times 10^{13}$ molecule cm^{-3} when the cross-sections of Bongartz et al. [51] are used;
- $(8.19 \pm 0.08) \times 10^{13}$ molecule cm^{-3} when the cross-sections of Stutz et al. [53] are used;
- $(1.00 \pm 0.01) \times 10^{14}$ molecule cm^{-3} when the cross-sections of Brust et al. [52] are used.

Using the simultaneous measurements made in our experiments, one can compare the UV and IR integrated band intensities (IBI) which are derived from the Beer–Lambert law. The IR integrated band intensities (IBI_{IR}) are calculated by

$$\int A_{IR}\, d\bar{\nu} = \int \sigma_{IR}\, d\bar{\nu} l_{IR} \times C \quad \text{with} \int \sigma_{IR}\, d\bar{\nu} = IBI_{IR}$$

Please cite this article as: Gratien A, et al. Experimental intercomparison of the absorption cross-sections of nitrous acid (HONO) in the ultraviolet and mid-infrared spectral regions. JQSRT (2008), doi:10.1016/j.jqsrt.2008.11.003

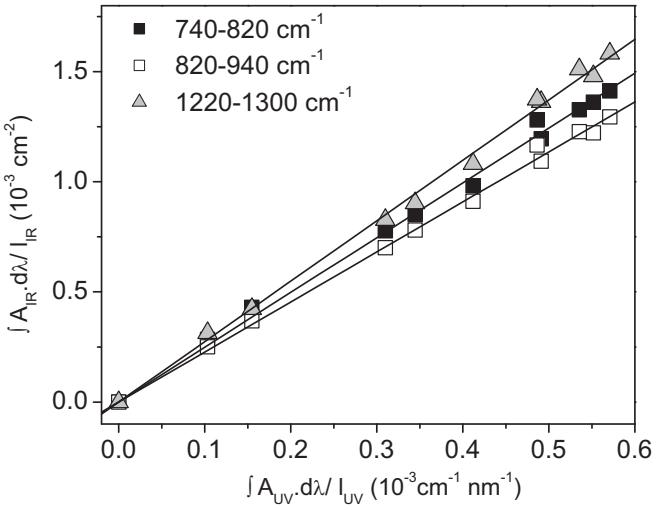

Fig. 3. IR versus UV integrated optical depths of nitrous acid. Ten inter-comparison experiments were performed by simultaneously acquiring UV and IR spectra, giving the ratios $IBI_{740-820\,cm^{-1}}/IBI_{325-390\,nm} = 2.49 \pm 0.12\,nm\,cm^{-1}$, $IBI_{820-900\,cm^{-1}}/IBI_{325-390\,nm} = 2.27 \pm 0.10\,nm\,cm^{-1}$, and $IBI_{1220-1300\,cm^{-1}}/IBI_{325-390\,nm} = 2.70 \pm 0.20\,nm\,cm^{-1}$. The errors quoted take into account the uncertainties in the linear regressions (2σ), those of the concentration determination estimated by the DOASIS software, as well as systematic errors (optical path lengths, stray light).

Table 2
Comparison of IR/UV integrated band intensities of this study with the ratio IBI_{IR}/IBI_{UV} derived from the IR/UV intercomparaison of Barney et al. [54, 55].

Spectral regions used for the integrated band intensities	This work	Barney et al. [54, 55]	Relative differences (%)
$IBI_{740-820\,cm^{-1}}/IBI_{325-390\,nm}$	2.49 ± 0.12	2.60 ± 0.50	4
$IBI_{820-900\,cm^{-1}}/IBI_{325-390\,nm}$	2.27 ± 0.10	2.32 ± 0.22	2
$IBI_{1220-1300\,cm^{-1}}/IBI_{325-390\,nm}$	2.70 ± 0.20	3.04 ± 0.32	12

Note: All ratios IBI_{IR}/IBI_{UV} are given in units of $(nm\,cm^{-1})$.

where A_{IR} is the IR absorbance (base e) at each wavenumber $\bar{\nu}$, σ_{IR} is the IR absorption cross-section at each wavenumber $\bar{\nu}$ (in $cm^2\,molecule^{-1}$), l_{IR} is the IR optical path length (in cm), and C is the HONO concentration (in $molecule\,cm^{-3}$).

The quantities $\int A_{IR} \times d\bar{\nu}/l_{IR}$ were calculated for the ten intercomparison experiments carried out in this study. The measured absorbances were integrated over the spectral regions 740–820, 820–900, and 1220–1300 cm^{-1}. In the UV region, the concentration of HONO was determined by the DOASIS software (see above) from each UV spectra recorded at the same time as the IR spectra. The average HONO concentrations multiplied by the average of the UV integrated band intensities ($IBI_{325-390\,nm}$) of Bongartz et al. [51], Stutz et al. [53], and Brust et al. [52] were calculated for the 10 experiments. According to the Beer–Lambert law, the average of $[HONO] \times IBI_{UV}$ is equal as $\int A_{UV} \times d\lambda/l_{UV}$ where A_{uv} is the UV absorbance (base e) at each wavelength λ and l_{UV} is the UV optical path length (in cm). In Fig. 3, the quantities $\int A_{IR} \times d\bar{\nu}/l_{IR}$ are plotted as a function of $\int A_{UV} \times d\lambda/l_{UV}$. According to the Beer–Lambert law, the slope of the straight line corresponds to the ratio IBI_{IR}/IBI_{UV} (in $nm\,cm^{-1}$). The intercomparison experiments give the ratios $IBI_{740-820\,cm^{-1}}/IBI_{325-390\,nm} = 2.49 \pm 0.12\,nm\,cm^{-1}$, $IBI_{820-900\,cm^{-1}}/IBI_{325-390\,nm} = 2.27 \pm 0.10\,nm\,cm^{-1}$ and $IBI_{1220-1300\,cm^{-1}}/IBI_{325-390\,nm} = 2.70 \pm 0.20\,nm\,cm^{-1}$. The internal consistency of the data of the present study is very good, about 2%, showing that the linearity of absorption is clearly fulfilled. The ratios IBI_{IR}/IBI_{UV} obtained in this work are then compared with the ratio IBI_{IR}/IBI_{UV} derived from the IR/UV intercomparaison of Barney et al. [54,55] (see Table 2). The errors quoted take into account the uncertainties on the linear regression (twice the standard deviation), those of the determination of the concentration by the DOASIS software, as well as systematic errors (optical path lengths, stray light). Consequently, the various ratios are known with an accuracy of 5%. This is sufficient to conclude on the coherence between IR and UV cross-sections because the HONO UV cross-sections published by Brust et al. [52] are about 22% smaller than those published by Stutz et al. [53] and Bongartz et al. [51].

4. Discussion

From the results of Table 2 it appears that there is good consistency between our intercomparison IR/UV and the study of Barney et al. [54,55] concerning the 740–820 and 820–900 cm^{-1} spectral regions. For the 1200–1300 cm^{-1} region, the two studies are consistent when taking into account the uncertainties (although a difference of about 12% is observed).

Please cite this article as: Gratien A, et al. Experimental intercomparison of the absorption cross-sections of nitrous acid (HONO) in the ultraviolet and mid-infrared spectral regions. JQSRT (2008), doi:10.1016/j.jqsrt.2008.11.003

Table 3
Integrated band intensities (IBI_{UV}) of HONO (in $10^{-18}\,cm^2\,molecule^{-1}\,nm^{-1}$) in the 325–390 nm spectral region.

IBI_{UV} obtained in this study using the IR reference data of		IBI_{UV} from the study of		
Kagann and Maki [57]	Hurley [56]	Bongartz et al. [51]	Brust et al. [52]	Stutz et al. [53]
5.9 ± 1.1	6.12 ± 0.70	6.24 ± 0.31	4.8 ± 0.4	5.9 ± 0.3

This difference can be explained by the subtraction procedure of residual water lines not carried out correctly in 1220–1300 cm^{-1} region as shown in Fig. 1. In the following, only the 740–900 cm^{-1} spectral region will be used for comparisons.

After having verified the agreement with the first IR/UV intercomparison of Barney et al. [54,55], one can now calculate the UV integrated band intensities ($IBI_{325-390\,nm}$), which are derived from the ratio IBI_{IR}/IBI_{UV} of this study and the available IR cross-sections of HONO in the 740–900 cm^{-1} region. Table 3 compares the UV integrated band intensities obtained in this work with the values available in the literature. The errors quoted take into account the uncertainties on the ratio IBI_{IR}/IBI_{UV} of this study and those of the IR cross-sections of HONO published in the literature. From the results of this table, the following observations can be made:

- The IR integrated band intensities by Kagann and Maki [57] and Hurley [56] are consistent when taking into account the uncertainties that are reflected in our different IBI_{UV} quoted in Table 3. Moreover, the study of Barney et al. [54,55] has demonstrated good agreement between the IR cross-sections of Kagann and Maki [57], Sakamaki et al. [58] and Hurley [56]. Consequently, one can conclude that there is an excellent agreement between the different IR studies.
- There are systematic differences between the different UV studies [51–53] that are reflected in the different UV integrated band intensities IBI_{UV} presented in Table 3. Indeed, the cross-sections published by Bongartz et al. [51] and by Stutz et al. [53] are about 22% higher than those published by Brust et al. [52].
- There is good consistency between the studies of Bongartz et al. [51] and of Stutz et al. [53] and the UV integrated band intensity IBI_{UV} of the present study, determined from the simultaneous infrared spectra together with the infrared integrated band intensities IBI_{IR} published by Hurley [56] and Kagann and Maki [57] when taking into account the uncertainties. Thus, our measurements support strongly the IUPAC [66] and JPL [67] databases that recommend the UV cross-sections of Bongartz et al. [51] and Stutz et al. [53], respectively.
- A difference of about 22% is observed between our IBI_{UV} and that published by Brust et al. [52]. If one assumes that the infrared data as well as our results are correct one can conclude that the UV cross-sections of Brust et al. [52] are underestimated by about 22%. The results of the present study confirm the intercomparison study of Kleffmann et al. [48] where the authors concluded that the cross-sections of Brust et al. [52] are most probably affected by some unknown errors. The reasons for this discrepancy are not perfectly clear but there is a possible artefact from the chemical quantification method (Kleffmann, private communication [68]) and a possible stray light problem with the used UV spectrometer (Kleffmann, private communication [69]).

In conclusion, the present study demonstrates that the UV cross-sections of Brust et al. [52] are too small by about 22% and that the UV cross-sections of Bongartz et al. [51] and of Stutz et al. [53] are in agreement with the different IR cross-sections to within 6%.

5. Implications for atmospheric chemistry

From the results of the present study it appears better to use the UV cross-sections of Bongartz et al. [51] or of Stutz et al. [53] in order to correctly measure atmospheric HONO or to calculate its photolysis rates. For example, it is the case in the study of Gherman et al. [32] which used the cross-sections of Stutz et al. [53] to measure nitrous acid by incoherent broadband cavity-enhanced absorption spectroscopy (IBBCEAS). Accordingly, the possible underestimation of the UV cross-sections of Brust et al. [52] has important consequences on atmospheric chemistry since these data are commonly used for atmospheric HONO measurements and for photolysis rate calculations. For example, Taylor et al. [70] used the cross-sections published by Brust et al. [52] to determine the initial concentration of OH radicals. Consequently, these experiments tend to underestimate the concentration of OH radicals.

Furthermore, in the intercomparison study by Kleffmann et al. [58], an excellent agreement was obtained between chemical methods (LOPAP, denuders) and DOAS. For the DOAS measurements in these comparisons, the cross-sections of Stutz et al. [53] were used. Although in the study published by Spindler et al. [42], the cross-sections of Stutz et al. [53] were also used, a factor of four higher concentrations between the denuder system and DOAS was observed. The difference is caused by chemical interferences of the denuder. Heland et al. [41] reported systematically lower (approximately 13%) concentrations of HONO measured by DOAS when performing intercomparison measurements with a LOPAP instrument, however the UV reference spectrum used to measure HONO by DOAS in this study is also the one published by Stutz et al. [53].

Please cite this article as: Gratien A, et al. Experimental intercomparison of the absorption cross-sections of nitrous acid (HONO) in the ultraviolet and mid-infrared spectral regions. JQSRT (2008), doi:10.1016/j.jqsrt.2008.11.003

Consequently, the difference is not caused by the HONO cross-section but by a NO_2 interference artefact in the DOAS instrument.

Concerning the photolysis rates and oscillator strength (i.e., integrated UV cross-sections), it is important to mention that very recently Wall et al. [59] proposed the absolute values of the UV absorption cross-sections of HONO as a potential source of systematic errors. More precisely, Wall et al. [59] suggested that the actual oscillator strength for the electronic bands of HONO should, on average, be 19.1% higher than the value reported by Bongartz et al. [50,51]. However, according to the present study, the HONO cross-sections of Bongartz et al. [51] are consistent with independent infrared studies and also in agreement to within 5% with the most recent UV cross-sections of Stutz et al. [53].

6. Conclusion

Simultaneous measurements of HONO absorption spectra in the IR and UV spectral ranges have been performed to evaluate the consistency of absorption cross-sections in both spectral regions. Our IR/UV intercomparison is in good agreement with that of Barney et al. [54,55]. Assuming that the infrared data are correct, this study shows that the Brust et al. [52] cross-sections are underestimated by about 22% and confirms that the UV cross-sections of Bongartz et al. [50,51] and of Stutz et al. [53] recommended by the JPL [67] and IUPAC [66] databases are indeed the most accurate ones.

Acknowledgements

This work has been supported by the French National Programme of Atmospheric Chemistry (PN-LEFE CHAT) and by the European Community within the 6th Framework Programme, section "Support for Research Infrastructure—Integrated Infrastructure Initiative": EUROCHAMP. The authors also thank IUP Heidelberg group for free access to DOASIS software. We wish to thank M. Hurley, J. Kleffmann, L. Wingen and B.J. Finlayson-Pitts for helpful discussions.

References

[1] Harrison RM, Peak JD, Collins GM. Tropospheric cycle of nitrous acid. J Geophys Res 1996;101:14,429–39.
[2] Alicke B, Geyer A, Hofzumahaus A, Holland F, Konrad S, Patz HW, et al. OH formation by HONO photolysis during the BERLIOZ experiment. J Geophys Res 2003;108:8247–64.
[3] Aumont B, Chervier F, Laval S. Contribution of HONO sources to the $NO_x/HO_x/O_3$ chemistry in the polluted boundary layer. Atmos Environ 2003;37:487–98.
[4] Kleffmann J, Gavriloaiei T, Hofzumahaus A, Holland F, Koppmann R, Rupp L, et al. Daytime formation of nitrous acid: a major source of OH radicals in a forest. Geophys Res Lett 2005;32:L05818.
[5] Acker K, Möller D, Wieprecht W, Meixner FX, Bohn B, Gilge S, et al. Strong daytime production of OH from HNO_2 at a rural mountain site. Geophys Res Lett 2006;33:L02809.
[6] Lammel G, Cape JN. Nitrous acid and nitrite in the atmosphere. Chem Soc Rev 1996;25:361–9.
[7] Febo A, Perrino C, Allegrini I. Measurement of nitrous acid in Milan, Italy, by DOAS and diffusion denuders. Atmos Environ 1996;30:3599–609.
[8] Harris GW, Carter WPL, Winer AM, Pitts Jr. JN, Platt U, Perner D. Observations of nitrous acid in the Los Angeles atmosphere and implications for predictions of ozone-precursor relationships. Environ Sci Technol 1982;16:414–9.
[9] Febo A, Perrino C. Measurement of high concentration of nitrous acid inside automobiles. Atmos Environ 1995;29:345–51.
[10] Calvert JG, Yarwood G, Dunker AM. An evaluation of the mechanism of nitrous acid formation in the urban atmosphere. Res Chem Intermediates 1994;20:463–502.
[11] Finlayson-Pitts BJ, Wingen LM, Sumner AL, Syomin D, Ramazan KA. The heterogeneous hydrolysis of NO_2 in laboratory systems and in outdoor and indoor atmospheres: an integrated mechanism. Phys Chem Chem Phys 2003;5:223–42.
[12] Vogel B, Vogel H, Kleffmann J, Kurtenbach R. Measured and simulated vertical profiles of nitrous acid—part II. Model simulations and indications for a photolytic source. Atmos Environ 2003;37:2957–66.
[13] Pagsberg P, Bjergbakke E, Ratajczak E, Sillesen A. Kinetics of the gas phase reaction OH+NO(+M)→ HONO(+M) and the determination of the UV absorption cross sections of HONO. Chem Phys Lett 1997;272:383–90.
[14] Chan WH, Nordstrom RJ, Calvert JG, Shaw JH. Kinetic study of HONO formation and decay reactions in gaseous mixtures of HONO, NO, NO_2, H_2O, and N_2. Environ Sci Technol 1976;10:674–82.
[15] Kurtenbach R, Becker KH, Gomes JAG, Kleffmann J, Lörzer JC, Spittler M, et al. Investigations of emissions and heterogeneous formation of HONO in a road traffic tunnel. Atmos Environ 2001;35:3385–94.
[16] Harrison RM, Kitto AMN. Evidence for a surface source of atmospheric nitrous acid. Atmos Environ 1994;28:1089–94.
[17] Reisinger AR. Observation of HNO_2 in the polluted winter atmosphere: possible heterogeneous production on aerosols. Atmos Environ 2000;34:3865–74.
[18] Saliba NA, Mochida M, Finlayson-Pitts BJ. Laboratory studies of sources of HONO in polluted urban atmospheres. Geophys Res Lett 2000;27:3229–32.
[19] Ammann M, Kalberer M, Jost DT, Tobler L, Rössler E, Piguet D, et al. Heterogeneous production of nitrous acid on soot in polluted air masses. Nature 1998;395:157–60.
[20] Arens F, Gutzwiller L, Baltensperger U, Gaggeler HW, Ammann M. Heteregenous reaction of NO_2 on diesel soot particles. Environ Sci Technol 2001;35:2191–9.
[21] Bröske R, Kleffmann J, Wiesen P. Heterogeneous conversion of NO_2 on secondary organic aerosol surfaces: a possible source of nitrous acid (HONO) in the atmosphere? Atmos Chem Phys 2003;3:469–74.
[22] Stemmler K, Ammann M, Donders C, Kleffmann J, George C. Photosensitized reduction of nitrogen dioxide on humic acid as a source of nitrous acid. Nature 2006;440:195–8.
[23] Stemmler K, Ammann M, Elshorbany Y, Kleffmann J, Ndour M, D'Anna B, et al. Light induced conversion of nitrogen dioxide into nitrous acid on submicron humic acid aerosol. Atmos Chem Phys Discuss 2007;7:4035–64.
[24] Zhou X, He Y, Huang G, Thornberry TD, Carroll MA, Bertman SB. Photochemical production of nitrous acid on glass sample manifold surface. Geophys Res Lett 2002;14:1681–5.

Please cite this article as: Gratien A, et al. Experimental intercomparison of the absorption cross-sections of nitrous acid (HONO) in the ultraviolet and mid-infrared spectral regions. JQSRT (2008), doi:10.1016/j.jqsrt.2008.11.003

[25] Lahoutifard N, Ammann M, Gutzwiller L, Ervens B, George C. The impact of multiphase reactions of NO_2 with aromatics: a modelling approach. Atmos Chem Phys 2002;2:215–26.
[26] George C, Strekowski RS, Kleffmann J, Stemmler K, Ammann M. Photoenhanced uptake of gaseous NO_2 on solid organic compounds: a photochemical source of HONO? Faraday Discuss 2005;130:195–210.
[27] Wennberg PO, Dabdub D. Rethinking ozone production. Science 2008;319:1624–5.
[28] Li S, Mathews J, Sinha A. Atmospheric hydroxyl radical production from electronically excited NO_2 and H_2O. Science 2008;319:1657–60.
[29] Platt U, Perner D. Detection of nitrous acid in the atmosphere by differential optical absorption. Geophys Res Lett 1979;6:917–20.
[30] Platt U, Perner D, Harris GW, Winer AM, Pitts Jr. JN. Observations of nitrous acid in an urban atmosphere by differential optical absorption. Nature 1980;285:312–4.
[31] Wang L, Zhang J. Detection of nitrous acid by cavity ring-down spectroscopy. Environ Sci Technol 2000;34:4221–7.
[32] Gherman T, Venables DS, Vaughan S, Orphal J, Ruth AA. Incoherent broadband cavity-enhanced absorption spectroscopy in the near-ultraviolet: application to HONO and NO_2. Environ Sci Technol 2008;42:890–5.
[33] Hanst PL, Wong NW, Bragin J. A long-path infrared study of Los-Angeles smog. Atmos Environ 1982;16:969–81.
[34] Tuazon EC, Winer AM, Graham RA, Pitts Jr. JN. Atmospheric measurements of trace pollutants by kilometers-pathlength FT-IR spectroscopy. Adv Environ Sci Technol 1980;10:259–300.
[35] Schiller CL, Locquiao S, Johnson TJ, Harris GW. Atmospheric measurements of HONO by tunable diode-laser absorption spectroscopy. J Atmos Chem 2001;40:275–93.
[36] Rodgers MO, Davis DD. A UV-photofragmentation/laser-induced fluorescence sensor for the atmospheric detection of HONO. Environ Sci Technol 1989;23:1106–12.
[37] Andrés-Hernandez MD, Notholt J, Hjorth J, Schrems O. A DOAS study on the origin of nitrous acid at urban and non-urban sites. Atmos Environ 1996;30:175–80.
[38] Sjödin A, Ferm M. Measurements of nitrous acid in urban area. Atmos Environ 1985;19:985–92.
[39] Febo A, Perrino C, Cortiello M. A denuder technique for the measurement of nitrous acid in urban atmospheres. Atmos Environ 1993;27A:1721–8.
[40] Simon PK, Dasgupta PK. Continuous automated measurement of gaseous nitrous and nitric acids and particulate nitrite and nitrate. Environ Sci Technol 1995;29:1534–41.
[41] Genfa Z, Slanina S, Boring CB, Jongejan PAC, Dasgupta PK. Continuous wet denuder measurements of atmospheric nitric and nitrous acids during the 1999 Atlanta supersite. Atmos Environ 2003;37:1351–64.
[42] Spindler G, Hesper J, Brüggemann E, Dubois R, Müller T, Herrmann H. Wet annular denuder measurements of nitrous acid: laboratory study of the artefact reaction of NO_2 with S(IV) in aqueous solution and comparison with field measurements. Atmos Environ 2003;37:2643–62.
[43] Kanda Y, Taira M. Chemiluminescent method for continuous monitoring of nitrous acid in ambient air. Anal Chem 1990;62:2084–7.
[44] Vecera Z, Dasgupta PK. Measurement of ambient nitrous acid and a reliable calibration source for gaseous nitrous acid. Environ Sci Technol 1991;25:255–60.
[45] Zhou X, Qiao H, Deng G, Civerolo K. A method for the measurement of atmospheric HONO based on DNPH derivatization and HPLC analysis. Environ Sci Technol 1999;33:3672–9.
[46] Huang G, Zhou X, Deng G, Qiao H, Civerolo K. Measurement of atmospheric nitrous acid and nitric acid. Atmos Environ 2002;36:2225–35.
[47] Heland J, Kleffmann J, Kurtenbach R, Wiesen P. A new instrument to measure gaseous nitrous acid (HONO) in the atmosphere. Environ Sci Technol 2001;35:3207–12.
[48] Kleffmann J, Lörzer JC, Wiesen P, Kern C, Trick S, Volkamer R, et al. Intercomparison of the DOAS and LOPAP techniques for the detection of nitrous acid (HONO). Atmos Environ 2006;40:3640–52.
[49] Appel BR, Winer AM, Tokiwa Y, Biermann H. Comparison of atmospheric nitrous acid measurements by annular denuder and differential optical absorption systems. Atmos Environ 1990;24A:611–6.
[50] Bongartz A, Kames J, Welter F, Schurath U. Near-UV absorption cross-sections and trans/cis equilibrium of nitrous acid. J Phys Chem 1991;95:1076–82.
[51] Bongartz A, Kames J, Schurath U, George C, Mirabel P, Ponche JL. Experimental determination of HONO mass accomodation coefficients using two different techniques. J Atmos Chem 1994;18:149–69.
[52] Brust AS, Becker KH, Kleffmann J, Wiesen P. UV absorption cross sections of nitrous acid. Atmos Environ 2000;34:13–9.
[53] Stutz J, Kim ES, Platt U, Bruno P, Perrino C, Febo A. UV–visible absorption cross sections of nitrous acid. J Geophys Res 2000;105:14585–92.
[54] Barney WS, Wingen LM, Lakin MJ, Brauers T, Stutz J, Finlayson-Pitts BJ. Infrared absorption cross-section measurements for nitrous acid (HONO) at room temperature. J Phys Chem 2000;104:1692–9.
[55] Barney WS, Wingen LM, Lakin MJ, Brauers T, Stutz J, Finlayson-Pitts BJ. Infrared absorption cross-section measurements for nitrous acid (HONO) at room temperature. Additions and corrections. J Phys Chem 2001;105:16.
[56] Hurley M. Private communication; 2007.
[57] Kagann RH, Maki AG. Infrared absorption intensities of nitrous acid (HONO) fundamental bands. JQSRT 1983;30:37–44.
[58] Sakamaki F, Hatakeyama S, Akimoto H. Formation of nitrous acid and nitric oxide in the heterogeneous dark reaction of nitrogen dioxide and water vapor in a smog chamber. Int J Chem Kinetics 1983;15:1013–29.
[59] Wall KJ, Schiller CL, Harris GW. Measurements of the HONO photodissociation constant. J Atmos Chem 2006;55:31–54.
[60] Doussin JF, Ritz D, Durand-Jolibois R, Monod A, Carlier P. Design of an environmental chamber for the study of atmospheric chemistry: new developments in the analytical device. Analysis 1997;25:236–42.
[61] Picquet-Varrault B, Orphal J, Doussin JF, Carlier P, Flaud JM. Laboratory intercomparison of the ozone absorption coefficients in the mid-infrared (10 μm) and ultraviolet (300–350 nm) spectral regions. J Atmos Chem A 2005;109:1008–14.
[62] Cox RA. Photolysis of nitrous acid in the presence of carbon monoxide and sulfur dioxide. J Photochem 1974;3:291–304.
[63] Orphal J. A critical review of the absorption cross-sections of O_3 and NO_2 in the 240–790 nm region. J Photochem Photobiol A 2003;157:185–209.
[64] Bogumil K, Orphal J, Homann T, Voigt S, Spietz P, Fleischmann OC, et al. Measurements of molecular absorption spectra with the SCIAMACHY pre-flight model: instrument characterization and reference data for atmospheric remote-sensing in the 230–2380 nm region. J Photochem Photobiol A 2003;157:167–84.
[65] Kraus S, Geyer A. DOASIS Jscript programming description. Institut fur Umweltphysik, University of Heidelberg; 2001. 〈http://www.iup.uni-heidelberg.de/bugtracker/projects/doasis/〉.
[66] Atkinson R, Baulch DL, Cox RA, Crowley JN, Hampson RF Jr., Kerr JA, et al. Summary of evaluated kinetic and photochemical data for atmospheric chemistry. IUPAC subcommittee on gas kinetic data evaluation for atmospheric chemistry, Web version July 2004.
[67] Sander SP, Golden DM, Kurylo MJ, Moortgat GK, Wine PH, Ravishankara AR, et al. Chemical kinetics and photochemical data for use in atmospheric studies. Evaluation Number 15. JPL Publication 06-2, Jet Propulsion Laboratory, Pasadena; 2006.
[68] Kleffmann J. Private communication; 2007.
[69] Kleffmann J. Private communication; 2005 (published in the MPI-Mainz-UV-VIS Spectral Atlas of gaseous molecules).
[70] Taylor PH, Yamada T, Neuforth A. Kinetics of OH radical reactions with dibenzo-p-dioxin and selected chlorinated dibenzo-p-dioxins. Chemosphere 2005;58:243–52.

Please cite this article as: Gratien A, et al. Experimental intercomparison of the absorption cross-sections of nitrous acid (HONO) in the ultraviolet and mid-infrared spectral regions. JQSRT (2008), doi:10.1016/j.jqsrt.2008.11.003